Published OnlineFirst December 30, 2015; DOI: 10.1158/0008-5472.CAN-15-2770

Microenvironment and Immunology

Cancer Research

STAT3 Establishes an Immunosuppressive Microenvironment during the Early Stages of Breast Carcinogenesis to Promote Tumor Growth and Metastasis

Laura M. Jones[1,2], Miranda L. Broz[3], Jill J. Ranger[1,2], John Ozcelik[2], Ryuhjin Ahn[4,5], Dongmei Zuo[1,2], Josie Ursini-Siegel[4,5], Michael T. Hallett[2], Matthew Krummel[3], and William J. Muller[1,2]

Abstract

Immunosurveillance constitutes the first step of cancer immunoediting in which developing malignant lesions are eliminated by antitumorigenic immune cells. However, the mechanisms by which neoplastic cells induce an immunosuppressive state to evade the immune response are still unclear. The transcription factor STAT3 has been implicated in breast carcinogenesis and tumor immunosuppression in advanced disease, but its involvement in early disease development has not been established. Here, we genetically ablated Stat3 in the tumor epithelia of the inducible PyVmT mammary tumor model and found that Stat3-deficient mice recapitulated the three phases of immunoediting: elimination, equilibrium, and escape. Pathologic analyses revealed that Stat3-deficient mice initially formed hyperplastic and early adenoma-like lesions that later completely regressed, thereby preventing the emergence of mammary tumors in the majority of animals. Furthermore, tumor regression was correlated with massive immune infiltration into the Stat3-deficient lesions, leading to their elimination. In a minority of animals, focal, nonmetastatic Stat3-deficient mammary tumors escaped immune surveillance after a long latency or equilibrium period. Taken together, our findings suggest that tumor epithelial expression of Stat3 plays a critical role in promoting an immunosuppressive tumor microenvironment during breast tumor initiation and progression, and prompt further investigation of Stat3-inhibitory strategies that may reactivate the immunosurveillance program. *Cancer Res; 76(6); 1416–28. ©2015 AACR.*

Introduction

Immunoediting refers to a three step process of interactions between the immune system and emerging cancer comprised of elimination, equilibrium, and escape (1, 2). During the elimination phase, antitumorigenic immune cells are involved in the eradication of cancerous lesions. This may be followed by a long period of equilibrium wherein cancerous cells are kept in check by the immune system. Eventually, these cancerous lesions escape through various mechanisms, which, though not well understood, can include cell-intrinsic alterations or the suppression or inactivation of the immune system (1, 2). Modulation of the tumor immune microenvironment is an important factor in tumor progression and disease outcome. Both a high CD4:CD8 T-cell ratio and/or elevated presence of intratumoral macrophages are associated with poor outcome and metastatic disease in human breast cancer (3–5) while higher Th1/Th2 ratios are excellent predictors of positive patient outcome (6). In addition, M2-macrophage polarization and metastasis has been shown to be induced by a Th2 response in murine models of breast cancer (7). However most of these studies focus on the immune microenvironment in invasive disease, leaving the mechanisms that promote antitumor immunity during the ductal carcinoma *in situ* (DCIS) to invasive disease transition poorly understood.

The transcription factor STAT3 has been observed to be constitutively active in 35% to 60% of human breast cancers (8, 9) as well as many other types of cancer (10, 11). In breast cancer, its expression and activation correlates with tumor grade, stage, presence of metastases and a higher risk of recurrence (8, 9). In addition, loss of Stat3 function has been shown to decrease tumor cell growth and angiogenesis, increase apoptosis *in vitro* (10) and decrease lung metastasis in a transgenic mouse model (12). Furthermore, Stat3 activation in the immune microenvironment is linked to the tumor-promoting effects of myeloid-derived suppressor cells (MDSC) and M2 tumor-associated macrophages (10, 13, 14). Stat3 activation has also been inversely correlated with immune cell infiltration *in vivo* (15–17) and its inactivation elicits antitumor immune responses in melanoma, lung cancer, and glioblastomas (15, 16). However, these studies mainly utilize xenograft models to examine Stat3-mediated

[1]Goodman Cancer Centre, McGill University, Montreal, Quebec, Canada. [2]Departments of Biochemistry, McGill University, Montreal, Quebec, Canada. [3]Department of Pathology, University of California San Francisco, San Francisco, California. [4]Department of Oncology, McGill University, Montreal, Quebec, Canada. [5]Lady Davis Institute, Jewish General Hospital, McGill University, Montreal, Quebec, Canada.

Note: Supplementary data for this article are available at Cancer Research Online (http://cancerres.aacrjournals.org/).

Corresponding Author: William Muller, Goodman Cancer Research Center, McGill University, Rm 507, 1160 Avenue des Pins Ouest, Montreal, Quebec H3A 1A3, Canada. Phone: 514-398-5847; Fax: 514-398-6769; E-mail: William.muller@mcgill.ca

doi: 10.1158/0008-5472.CAN-15-2770

immune suppression in advanced disease, leaving its interactions at tumor initiation largely unexplored.

In this study, we investigated the role of Stat3 in mammary tumor progression by crossing conditional Stat3 ($Stat3^{flx}$) mice (18) with a mouse model of mammary tumor progression that expresses the Polyomavirus middle T (PyVmT) and Cre recombinase (Cre) in a doxycycline-inducible fashion (MMTV-MTB/TetO-MIC; ref. 19). This novel model allows for a temporal analysis of tumor initiation and progression. Mammary epithelial-specific disruption of Stat3 resulted in a profound delay in mammary tumor onset and penetrance. In addition, the Stat3-deficient tumors that eventually emerged demonstrated a major metastatic defect. Despite this delay in tumor onset, mammary epithelial ablation of Stat3 did not prevent the initiation of early hyperplastic lesions in these mice. However these lesions were rapidly cleared by a robust immune response, driven by myeloid and T-cell populations. Furthermore, the Stat3-deficient tumors lacked a transcriptional program involved in proinflammatory recruitment of myeloid cells and implicated in metastatic progression. Together, these observations recapitulate all three stages of the immunoediting program and indicate that Stat3 promotes an immunosuppressive tumor microenvironment involved in modulating early tumor outgrowth and later stages of metastasis.

Materials and Methods

Transgenic mice

Onset of mammary tumors was determined by biweekly physical palpation. Animals were sacrificed at predetermined time points postinduction of doxycycline treatment (2 mg/mL in drinking water) or at an ethical maximum tumor burden. Tumor, mammary gland, and lung material was frozen in liquid nitrogen, set in optimal cutting temperature (OCT) medium then frozen or fixed with either 10% neutral buffered formalin or a commercially available zinc fixative (BD Pharmingen: 550523) and embedded in paraffin. The fixed and embedded materials were sectioned at 4 μm and stained by hematoxylin and eosin (H&E) or processed as indicated below. Metastatic lesions were detected and scored by sectioning the lungs at 50 μm intervals and stained for H&E.

Immunoblotting, immunofluorescent, and immunohistochemical analyses

Frozen mammary tumors were lysed using a PLC-γ buffer and run on SDS-PAGE gels. Immunofluorescent and immunohistochemical analyses were performed on paraffin or OCT-embedded sections as described previously (12). Staining was quantified when indicated using slides scanned with a Scanscope XT Digital Slide Scanner (Aperio) and corresponding positive pixel and nuclear immunohistochemical algorithms.

Flow cytometry

All antibodies were purchased from BD Pharmingen, eBioscience, Invitrogen, BioLegend, the UCSF hybridoma core, or were produced in the Krummel's laboratory. For surface staining, cells were incubated with anti-Fc receptor antibody (clone 2.4G2) and stained with antibodies in PBS + 2% FCS for 30 minutes on ice. Viability was assessed by staining with fixable Live/Dead Zombie (BioLegend) or DAPI. All flow cytometry was performed on a BD Fortessa flow cytometer. Analysis of flow cytometry data was done using Flowjo (Treestar).

qRT-PCR

qRT-PCR was performed using a Roche LC480 SYBR Green RT-PCR Kit (Roche). Samples were run using a LightCycler (Roche) and each reaction was run in triplicate. The resulting crossing point values were normalized against GAPDH to generate the relative transcript levels using the formula: $2^{\wedge}$(average GAPDH crossing point − average target × crossing point).

Microarray results have been deposited in the Gene Expression Omnibus database under the accession number GSE75325.

Supplementary information

Additional information can be found in Supplementary Materials and Methods.

Results

Stat3 loss results in a significant delay in mammary tumorigenesis

To evaluate the role of Stat3 in PyVmT-driven tumor progression, we interbred the conditional Stat3 strain (18) with mice carrying the MMTV-rtTA (MTB; ref. 20) and the inducible TetO-PyVmT-IRES-Cre recombinase (MIC; ref. 19) transgenes. This doxycycline-inducible PyVmT model couples the expression of the PyVmT oncogene and Cre, and subsequent deletion of the conditional *Stat3* allele(s), specifically in the mammary epithelium upon induction with doxycycline (Fig. 1A). Cohorts of virgin female mice bearing the wild type, one conditional or both conditional *Stat3* alleles ($Stat3^{wt/wt}$/MTB/MIC, $Stat3^{wt/flx}$/MTB/MIC, and $Stat3^{flx/flx}$/MTB/MIC) were generated. Whereas the $Stat3^{wt/wt}$/MTB/MIC and $Stat3^{wt/flx}$/MTB/MIC mice developed mammary tumors with an average onset of 20 or 28 days, respectively, the Stat3-deficient MIC mice displayed a significant delay in tumor onset to an average of 275 days (Fig. 1B). Furthermore, the $Stat3^{flx/flx}$/MTB/MIC mice demonstrated a decrease in tumor penetrance, as only 31% developed tumors compared with 80% and 73% of the $Stat3^{wt/wt}$/MTB/MIC and $Stat3^{wt/flx}$/MTB/MIC mice, respectively. We confirmed *Stat3* ablation and oncogene expression by PCR (Supplementary Fig. S1A), immunoblot and IHC (Fig. 1C and D). Total levels of Stat3 and its activated form (Stat3-pY705) were significantly reduced in the Stat3-deficient tumors. In addition to a similar average onset, the tumors from the $Stat3^{wt/flx}$/MTB/MIC mice expressed similar levels of Stat3 protein and activation to the parental MIC tumors (data not shown). Residual Stat3 protein observed in both the immunoblot and immunohistochemical staining (Fig. 1C and D) is a result of Stat3 retention in the stroma and tumor-infiltrating cells. The epithelial specificity of the Stat3 ablation was confirmed by immunofluorescence and immunohistochemical staining (Supplementary Fig. S1B and S1C). Histologic analysis of end-stage tumors from all genotypes revealed a similar solid adenocarcinoma phenotype. Thus, the mammary epithelial ablation of Stat3 delays tumor onset and decreases penetrance, suggesting a requirement for additional cooperating events.

Stat3 is dispensable for the initial outgrowth of PyVmT hyperplasias but is critical for their immune evasion

An advantage of the PyVmT tumor model is the ability to investigate tumor progression through distinct phases from early mammary hyperplasias and adenomas to end-stage adenocarcinomas (19). To evaluate these early stages, we performed histologic analyses on the transformed mammary glands after 2, 4, and

Published OnlineFirst December 30, 2015; DOI: 10.1158/0008-5472.CAN-15-2770

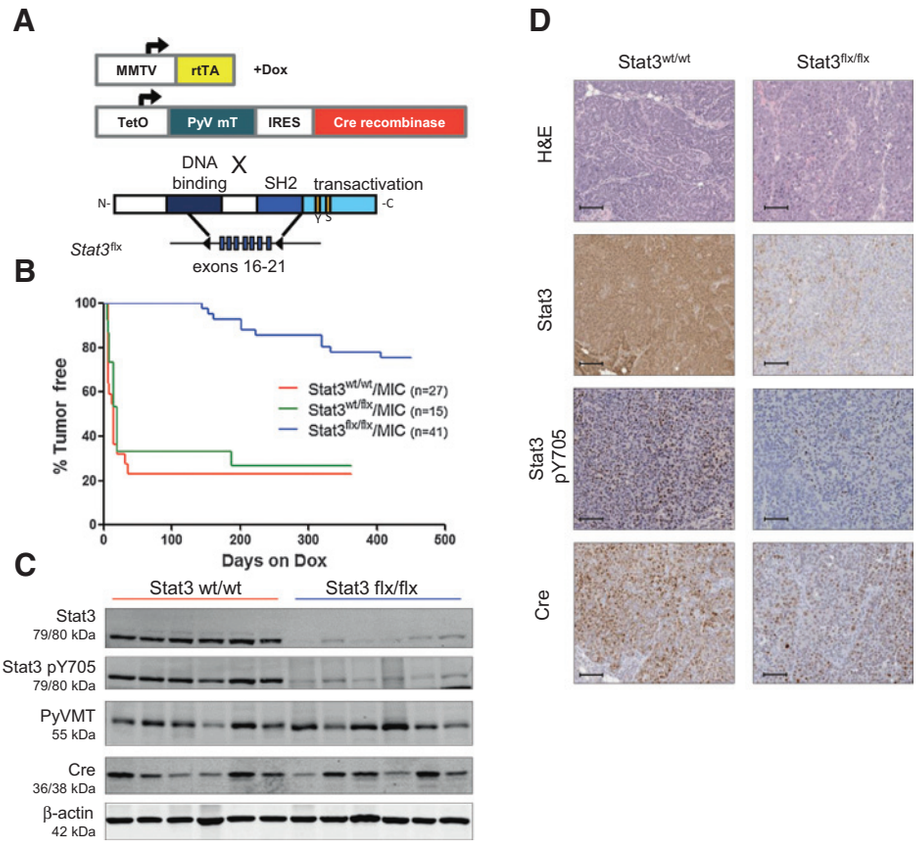

Figure 1.
Stat3 ablation results in a significant delay in mammary tumorigenesis. A, schematic of MMTV-rtTA, TetO-MIC, and *Stat3* flx transgenes. B, mammary tumor onset in $Stat3^{wt/wt}$/MTB/MIC, $Stat3^{wt/flx}$/MTB/MIC, and $Stat3^{flx/flx}$/MTB/MIC cohorts (T50 = 20, 28, 275 days, respectively). C, immunoblot analysis of Stat3, Cre, and PyVmT expression in mammary tumor cell lysates from $Stat3^{wt/wt}$/MTB/MIC and $Stat3^{flx/flx}$/MTB/MIC animals. D, staining of paraffin-embedded sections of mammary tumors by H&E (top) or using antibodies against Stat3 and Stat3-Y705P (middle rows) or Cre (bottom). Scale bar, 100 μm.

6 weeks of doxycycline induction. These analyses revealed that the $Stat3^{flx/flx}$/MTB/MIC mice developed mammary epithelial hyperplasias and adenomas with 100% penetrance comparable with their Stat3-proficient counterparts, albeit involving a lower proportion of the mammary epithelial tree (Fig. 2A, top; Supplementary Fig. S2A–S2C). These Stat3-deficient lesions had begun to regress by the fourth week of induction (Fig. 2A, middle). Remarkably, by 6 weeks of induction, the Stat3-deficient mammary glands were completely devoid of hyperplasias or adenomas, whereas Stat3-proficient glands exhibited invasive adenocarcinomas (Fig. 2A, bottom). We confirmed mammary epithelial deletion of Stat3 by both immunohistochemical (Fig. 2B) and immunofluorescence analyses (Supplementary Fig. S2D).

Given that Stat3 has been implicated in the proliferative capacity of mammary tumors and cancer cell lines (10–12), we examined the proliferative or apoptotic profiles of these Stat3-deficient lesions by staining for Ki67 as a proliferative marker and cleaved caspase-3 and terminal deoxynucleotidyl transferase–mediated dUTP nick end labeling (TUNEL) as markers of apoptosis. Neither the proliferative nor apoptotic status of the Stat3-deficient lesions was altered between genotypes after 2 weeks of induction (Fig. 2C). Taken together, these findings suggest that Stat3 is not necessary for the initiation of these early lesions but is crucial for their progression to invasive carcinomas.

Another explanation for the regression of the Stat3-deficient lesions is clearance by an activated immune response. It should be noted that although 100% of MIC animals develop mammary epithelial hyperplasias, only 80% develop end-stage tumors. To investigate this we used both IHC and flow cytometry to identify the nature of the immune infiltrate to these lesions. Initially, we examined the extent of overall leukocyte infiltration as well as specific myeloid components. Immunohistochemical analyses revealed that Stat3-deficient lesions were preferentially enriched in both $CD45^+$ leukocyte and $F4/80^+$ macrophage populations that circumscribed the emerging Stat3-deficient lesions ($CD45^-$ $Stat3^{wt/wt}$ 20.96% ± 2.80% vs. $Stat3^{flx/flx}$ 31.33% ± 2.49%, $F4/80^-$ $Stat3^{wt/wt}$ 16.67% ± 1.77% vs. $Stat3^{flx/flx}$ 27.95% ± 1.59%; Fig. 3A). Given that $CD45^+$ population is comprised of a plethora of distinct immune effector cells, we utilized flow cytometric analyses to distinguish between specific cell populations. We initially sorted the $CD45^+$ cells on CD11b (myeloid-specific marker) and Ly6C (monocyte marker) expression. Ly6C-negative cells were gated on $MHCII^+$ expression and further distinguished by F4/80hi, CD24lo expression (macrophages), and CD24hi, F4/80lo expressers (dendritic cells, DC). Macrophages were divided on the basis of differential expression of CD11c and CD11b and are here identified as TAM1 (CD11clo, CD11bhi) and TAM2 (CD11chi, CD11blo; Fig. 3B). These macrophage populations correspond to similarly delineated MHCIIlo (TAM1) and MHCIIhi (TAM2) populations, where CD11c high TAM2 macrophages display classically activated M1 gene signatures (21). DCs were subgated into two populations based on CD11b and CD103 expression as described previously (Fig. 3C; ref. 22). Consistent with the immunohistochemical data, we found that the $CD45^+$ compartment was dramatically enriched in the Stat3-deficient mammary glands after 2 weeks of induction ($Stat3^{wt/wt}$ 49.43% ± 6.64% vs.

Published OnlineFirst December 30, 2015; DOI: 10.1158/0008-5472.CAN-15-2770

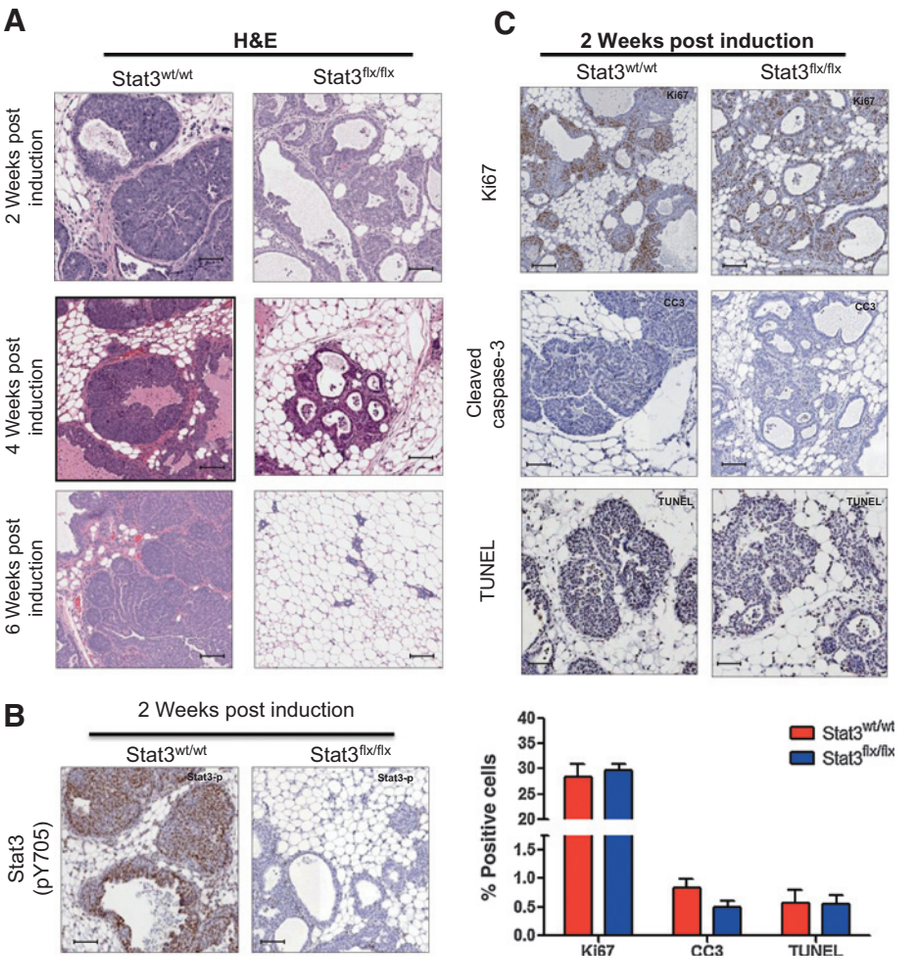

Figure 2.
Stat3 is not required for the initiation of mammary lesions, but is important for tumor progression. A, paraffin-embedded sections of mammary glands and tumors after 2, 4, and 6 weeks of doxycycline induction, stained by H&E. B, mammary glands after 2 weeks of doxycycline induction stained using antibodies against Stat3-pY705 to confirm Stat3 ablation. C, mammary glands after 2 weeks of doxycycline induction stained using antibodies against Ki67 (top), cleaved caspase-3 (middle), or TUNEL (bottom). Quantification of the positive nuclear staining of Ki67, cleaved caspase-3, and TUNEL stains. Scale bar, 100 μm; $n = 10$ biologic replicates per genotype. CC3, cleaved caspase-3.

$Stat3^{flx/flx}$ 71.90% ± 1.33%; Fig. 3D). Interestingly, we did not see such a dramatic difference in $F4/80^+$ macrophages by FACS ($Stat3^{wt/wt}$ 10.65% ± 2.88% vs. $Stat3^{flx/flx}$ 11.89% ± 0.84%; Fig. 3B and D). However, there was a shift towards TAM2 macrophages in the Stat3-deficient glands. One marker of the protumorigenic M2 class of macrophages is CD206 (the mannose receptor; ref. 23). Consistent with the protumorigenic role of M2 macrophages, the Stat3-deficient lesions exhibited a marked decrease in CD206 expression in the TAM1 macrophage population compared with the macrophages found in their Stat3-proficient counterparts (Fig. 3B and E). DCs are another key myeloid population that modulates T-cell responses in cancer (22, 24, 25). Consistent with the antitumor function of the CD103 subclass of DCs, the Stat3-deficient lesions exhibited a significant increase in the ratio of $CD103^+$ DCs to $CD11b^+$ DCs (CD103:CD11b ratio of 2.10 ± 0.17) compared with Stat3-proficient lesions (CD103:CD11b ratio of 0.69 ± 0.11; Fig. 3D). Taken together, these observations argue that the loss of Stat3 in the tumor epithelia results in an increase of antitumor myeloid populations in these lesions.

T-cell populations work in concert with these myeloid cells to elicit an antitumor immune response. To identify the nature of the T-cell infiltrates, we again employed both IHC and flow cytometry, utilizing various T-cell–specific markers. Using CD3ε as a pan T-cell marker, we observed a dramatic increase in the number of $CD3^+$ T cells to the Stat3-deficient lesions relative to wild-type counterparts ($Stat3^{flx/flx}$ 10.41% ± 1.88% vs. $Stat3^{wt/wt}$ 2.14% ± 0.37%; Fig. 4A). The observed increase in the CD3 population was comprised of an increase in both the $CD4^+$ [regulatory T (Tregs) and effector T cells (Teff)] and $CD8^+$ (CTLs) T-cell subsets in the Stat3-deficient lesions (CD4+ $Stat3^{wt/wt}$ 6.79% ± 0.80% vs. $Stat3^{flx/flx}$ 19.66% ± 1.59%, $CD8^+$ $Stat3^{wt/wt}$ 1.34% ± 0.25% vs. $Stat3^{flx/flx}$ 6.28% ± 0.97%; Fig. 4A). Furthermore, we utilized a progressive gating strategy to evaluate the activation status of the different T-cell populations. The $CD45^+$ compartment was isolated, then gated on the basis of $CD90.1^+$ (T-cell marker) expression. T-cell populations were further divided on the basis of CD8 (CTLs) and CD4 expression, which was further divided into $CD4^+$ $Foxp3^+$ (Tregs) and $CD4^+$ $Foxp3^-$ (Teff) populations. The activation status of each of these T-cell populations was further assessed using CD44 and PD1 as markers of activation (Fig. 4B and D). These flow cytometric analyses revealed that the Stat3-deficient mammary lesions have elevated levels of $CD8^+$ CTLs ($Stat3^{flx/flx}$ 8.96% ± 1.43 vs. $Stat3^{wt/wt}$ 3.03% ± 0.96; Fig. 4B and C). While both genotypes showed similar levels of activated effector T cells, there was a trend towards a decrease in activated Tregs in the Stat3-deficient mammary lesions and

Published OnlineFirst December 30, 2015; DOI: 10.1158/0008-5472.CAN-15-2770

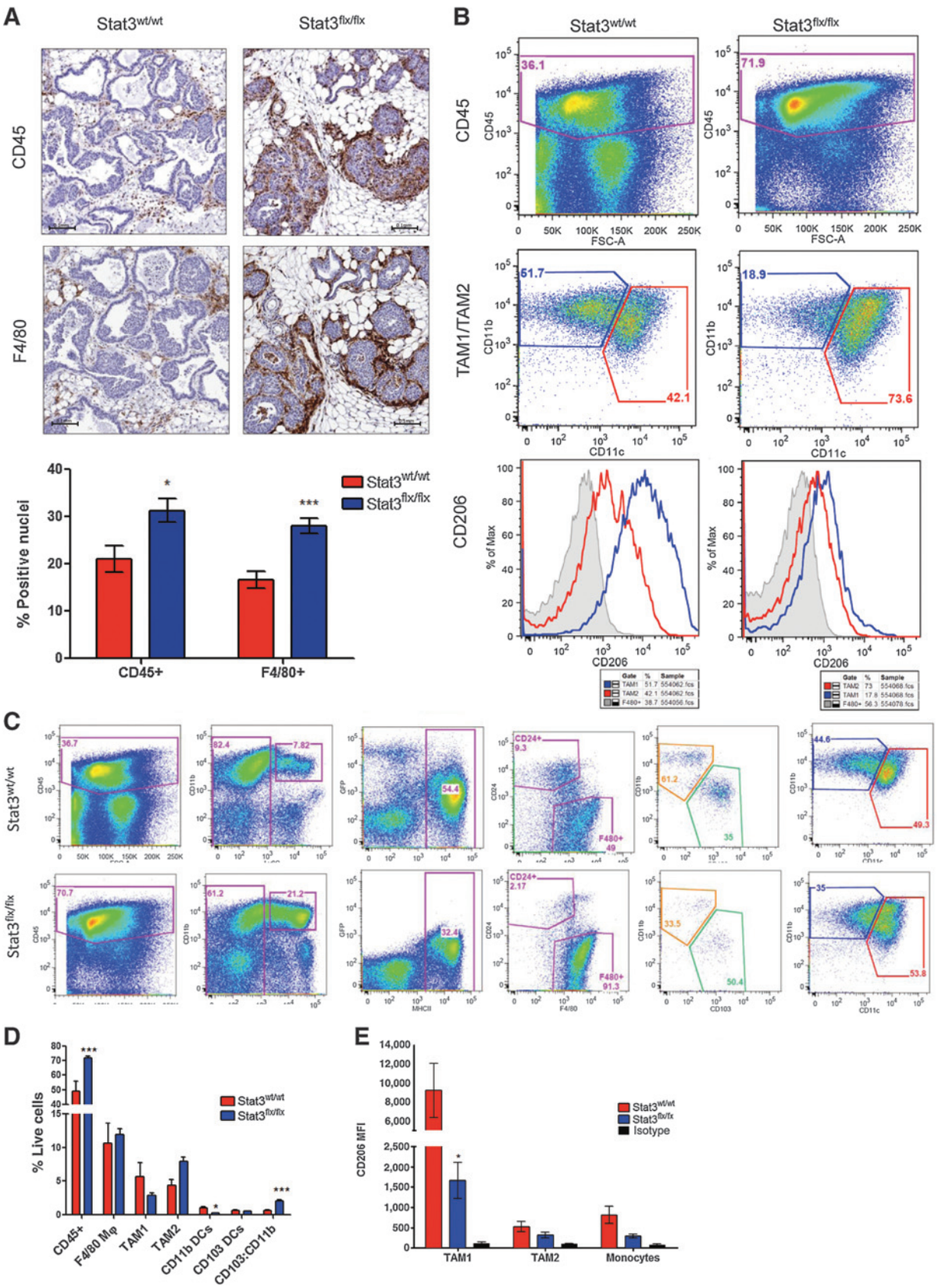

Published OnlineFirst December 30, 2015; DOI: 10.1158/0008-5472.CAN-15-2770

more significantly a substantial increase in activated CTLs ($Stat3^{wt/wt}$ 0.45% ± 0.02 vs. $Stat3^{flx/flx}$ 3.26% ± 0.67; Fig. 4D). Given that a high CD8:CD4 ratio is indicative of an antitumor response (6), we examined this relationship in the Stat3-deficient lesions and found they exhibited a significant increase in CD8:CD4 ratios (CD8:CD4 ratio $Stat3^{flx/flx}$ 1.35 ± 0.21 vs. $Stat3^{wt/wt}$ 0.53 ± 0.07; Fig. 4C). When activation status of these T-cell populations was taken into account, the activated CD8:activated CD4 ratio was even more strikingly elevated in the Stat3-deficient lesions (actCD8:actCD4 ratio $Stat3^{flx/flx}$ 4.37 ± 0.78 vs. $Stat3^{wt/wt}$ 0.32 ± 0.03; Fig. 4D). Collectively, these observations indicate that tumor epithelial expression of Stat3 plays a critical role in establishing immunosuppressive tumor microenvironment early in tumor development.

The T-cell compartment is involved in early stages of immune surveillance of the Stat3-deficient lesions

Although we have shown that loss of Stat3 in emerging hyperplasias results in the rapid recruitment of both myeloid and T-cell populations, the relative contribution of each these immune infiltrates to the immune clearance is unclear. To directly investigate the contribution of the T-cell compartment, we introduced both the Stat3-proficient and deficient MIC lines onto the SCID genetic background, which lacks both B and T cells (26). After a 6-week doxycycline induction, we examined the glands by histology. This showed that, in contrast to the invasive adenocarcinomas exhibited by the Stat3-proficient tumors, the Stat3-deficient lesions were primarily comprised of hyperplasia-like lesions in the immunodeficient SCID background (Fig. 5A, bottom). Notably, at this stage of induction, on immunocompetent FVB genetic background, the Stat3-deficient PyVmT lesions have become completely cleared (Figs. 5A, top and 2A, bottom). Despite the difference in histologic grades between the Stat3-deficient and proficient SCID backgrounds, both sets of lesions exhibited a similar proliferative and apoptotic status (Fig. 5B). While loss of the T- and B-cell compartment rescued the hyperplastic phase of tumor progression, infiltration of non-T- and B-cell immune cell types was still significantly increased to the Stat3-deficient lesions as assessed immunohistochemically with leukocyte and macrophage markers (CD45 and F4/80, respectively), relative to their wild-type counterparts (CD45, $Stat3^{flx/flx}$ 10.69% ± 1.21% vs. $Stat3^{wt/wt}$ 3.33% ± 0.70%; F4/80, $Stat3^{flx/flx}$ 4.59% ± 1.04% vs. $Stat3^{wt/wt}$ 1.10% ± 0.19%; Fig. 5C). Collectively, these observations indicate that full clearance of Stat3-deficient lesions requires an active adaptive immune response. However, given that Stat3-deficient PyVmT lesions did not fully evolve into invasive adenocarcinomas, the Stat3-deficient tumor cells may still be susceptible to the remaining immune populations to limit malignant progression.

A Stat3-dependent inflammatory network is required for the metastatic phase of PyVmT tumor progression

Previous studies with a MMTV-driven ErbB2 model of mammary tumorigenesis have demonstrated that, while mammary epithelial ablation of Stat3 does not impact the induction of ErbB2 mammary tumors, metastasis of these tumors to the lungs is severely impaired (12). To evaluate whether activation of Stat3 plays a similar role in the inducible PyVmT model, we took the lungs of tumor-bearing mice from both the Stat3-proficient and deficient strains at the same tumor burden and scored them for metastatic lesions. Strikingly, none of the Stat3-deficient tumor bearing animals developed lung metastases compared with 100% of their Stat3-proficient counterparts (Fig. 6A and C). Interestingly, although all the tumor-bearing PyVmT mice heterozygous for the Stat3 conditional allele did develop lung metastases, the lungs had, on average, fewer metastatic lesions compared with the wild-type mice ($Stat3^{wt/wt}$ 65.17 ± 16.61 vs. $Stat3^{wt/flx}$ 8.75 ± 3.80; Fig. 6B). To assess whether this metastatic defect was due to an inability to extravasate or a difficulty colonizing a secondary site, we injected freshly dissociated tumors directly into the vasculature of NCr mice. In the absence of any immunosurveillance, the Stat3-deficient cells were still unable to colonize the lungs to the same extent as their wild-type counterparts (Supplementary Fig. S3A–S3C). This suggests an inability of the Stat3-deficient tumors to develop a metastatic niche, survive, and grow in the lungs, independent of an active immune response.

To investigate this metastatic defect, we compared the gene expression profiles of the Stat3-proficient and deficient tumors. The results revealed that the Stat3-deficient tumors exhibited a significant decrease in many proinflammatory genes that are both Stat3 transcriptional targets and are functionally involved in the metastatic cascade (Fig. 6D), many of which we have previously identified in a MMTV-driven ErbB2 model (12). For example C/EBPδ and oncostatin M receptor (OSMR), which are known to potentiate the acute phase response (APR; refs. 27, 28), are significantly downregulated in Stat3-deficient tumors. Interestingly, other downregulated genes in the Stat3-deficient tumors include the serum amyloid A genes, *Saa1*, *Saa2*, and *Saa3*, which are known transcriptional targets of both C/EBPδ and Stat3 through its binding interaction with NFκB transcription factor (29–31). Additional genes involved in inflammation and metastasis were significantly downregulated in Stat3-deficient tumors including *Gata2* (5.8-fold), *Bcl3* (2.2-fold), *Spp1* (3.7-fold), and *Rb1* (2.5-fold; Fig. 6D).

To confirm the gene expression profiling data, we performed quantitative real-time PCR (qRT-PCR) on total RNA extracted from the Stat3-proficient and deficient tumors on these key Stat3 target genes. After establishing significantly reduced *stat3* transcript levels in the Stat3-deficient tumors compared with the wild-type tumors (19 fold decrease), we established that the expression levels of *Cebpd* and *Osmr* were also downregulated (5.7- and 5.2-

Figure 3.

Stat3 is crucial for tumor immune evasion. Specific myeloid populations are increased in the absence of Stat3. A, paraffin-embedded sections of mammary glands after 2 weeks of induction stained for total leukocytes (CD45, top) and macrophages (F4/80, bottom) with quantification of positive cell staining; $n = 8$ biologic replicates per genotype. Scale bar, 100 μm. B–E, flow cytometric analysis of immune infiltrate after 2 weeks of induction (representative of two independent trials, $Stat3^{wt/wt}$ $n = 3$, $Stat3^{flx/flx}$ $n = 6$ biologic replicates). B, representative flow plots for gating of total leukocytes (CD45, top) and macrophage populations [TAM1/TAM2 ($CD45^+$, $Ly6C^-$, $MHCII^+$, $F4/80^+$), middle; TAM1 and CD206, bottom). C, representative flow gating of DCs including CD11b and CD103 populations. D, quantification of total leukocytes (CD45), macrophage populations (TAM1, TAM2), DC populations (CD11b, CD103), and DC ratio (CD103:CD11b). E, quantification of CD206 mean fluorescent intensity (MFI) in TAM1, TAM2, and monocyte populations (statistical significance determined by Student *t* test, *, $P < 0.05$; ***, $P < 0.001$).

Published OnlineFirst December 30, 2015; DOI: 10.1158/0008-5472.CAN-15-2770

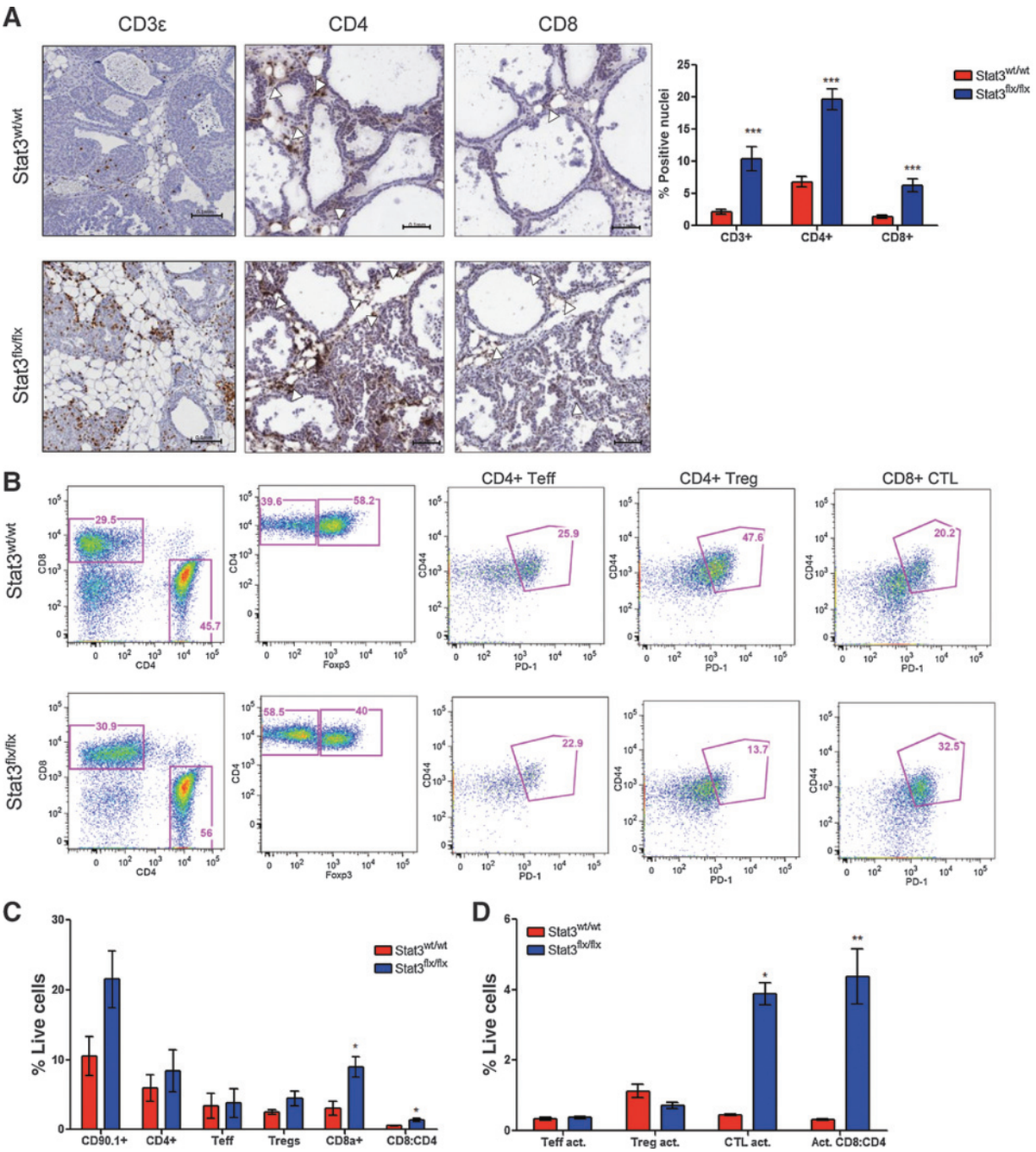

Figure 4.
Loss of Stat3 increases T-cell recruitment and activation. A, paraffin-embedded sections of mammary glands after 2 weeks of induction stained for total T cells (CD3, left), $CD4^+$ T cells (CD4, middle), and CTLs (CD8, right) with quantification; $n = 8$ biologic replicates per genotype; scale bar, 100 μm. B–D, flow cytometric analysis of T-cell immune infiltrate after 2 weeks of induction (representative of two independent trials, $Stat3^{wt/wt}$ $n = 3$, $Stat3^{flx/flx}$ $n = 6$ biologic replicates). B, representative gating of T-cell populations and activation. C, quantification of total T cells (CD90.1), T effector (Teff) cells ($CD4^+$, $FoxP3^-$), T regulatory (Treg) cells ($CD4^+$, $FoxP3^+$), CTLs (CD8+), and CD8:CD4 T-cell ratio. D, quantification of T-cell activation status based on double positivity for CD44 and PD1 within the T-cell populations as well as activated CD8:activated CD4 ratio (*, $P < 0.05$; **, $P < 0.01$).

fold, respectively) in the Stat3-deficient tumors (Fig. 6D). Consistent with the array data, the Stat3-deficient tumors exhibited a dramatic downregulation of the transcript levels of *Saa1*, *Saa2*, *Saa3*, and *S100a8*. (Fig. 6D).

Given that many of the downregulated Stat3 target genes are involved in promoting a proinflammatory tumor microenvironment, we investigated whether the Stat3-deficient tumors exhibited a deficit in immune infiltrates. To accomplish this, we stained

Published OnlineFirst December 30, 2015; DOI: 10.1158/0008-5472.CAN-15-2770

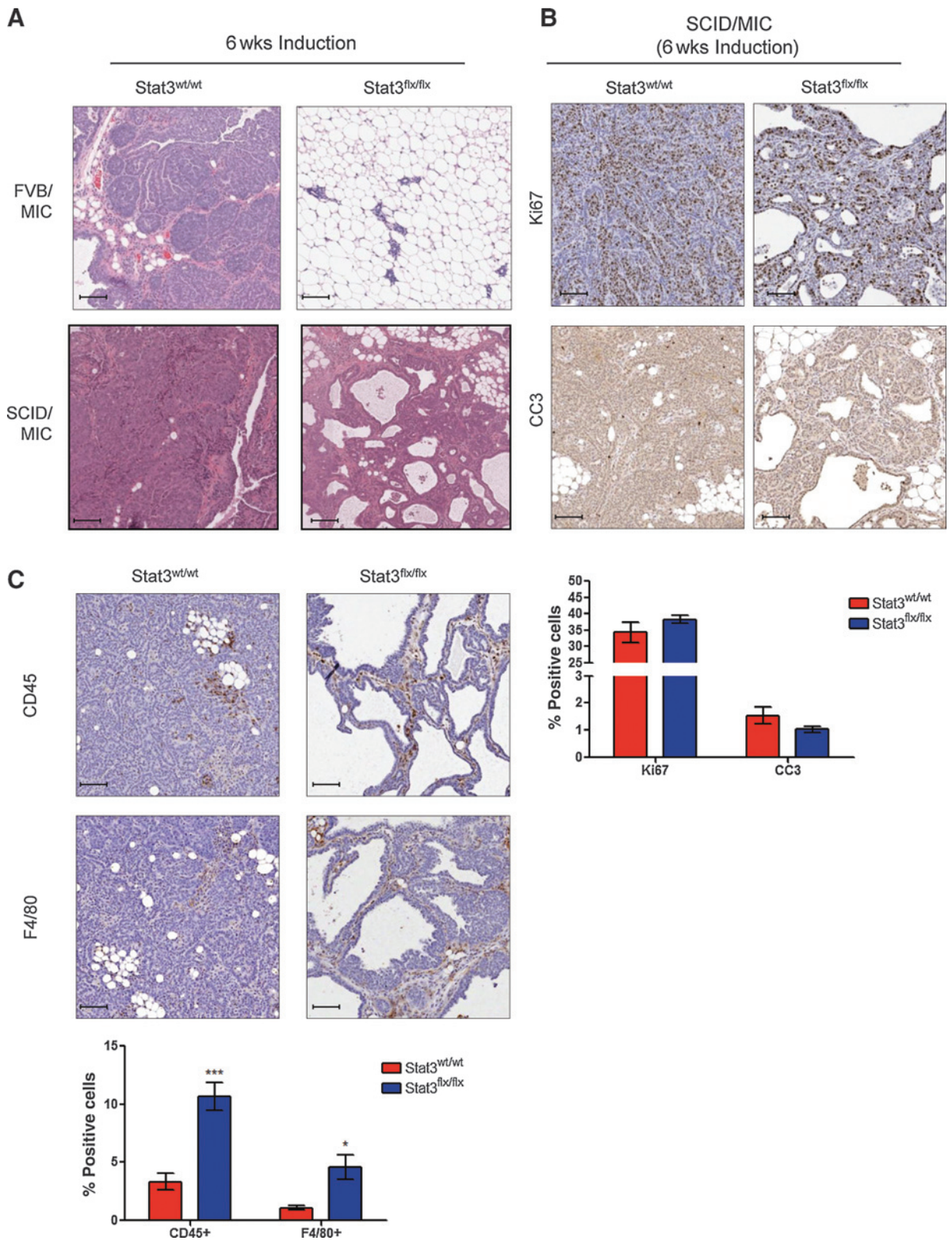

Figure 5.
Loss of the T-cell compartment partially rescues clearance of the Stat3$^{flx/flx}$ early lesions. A, staining of paraffin-embedded sections of mammary tumors or mammary glands by H&E after 6 weeks of induction. Top images are representative of mice bred on a fully immunocompetent background (FVB). Bottom images are representative of mice bred to a SCID/FVB background, which lacks all T and B cells. B, mammary tumors/glands after 6 weeks of doxycycline induction stained using antibodies against Ki67 (top) and cleaved caspase 3 (bottom). Quantification of the positive nuclear staining. C, mammary tumor/gland sections stained for total leukocytes (CD45, top) and macrophages (F4/80, bottom). Quantification of the positive nuclear staining (*, $P < 0.05$; ***, $P < 0.001$). Scale bar, 100 μm. IHC, $n = 8$ tumors per genotype. CC3, cleaved caspase-3.

Published OnlineFirst December 30, 2015; DOI: 10.1158/0008-5472.CAN-15-2770

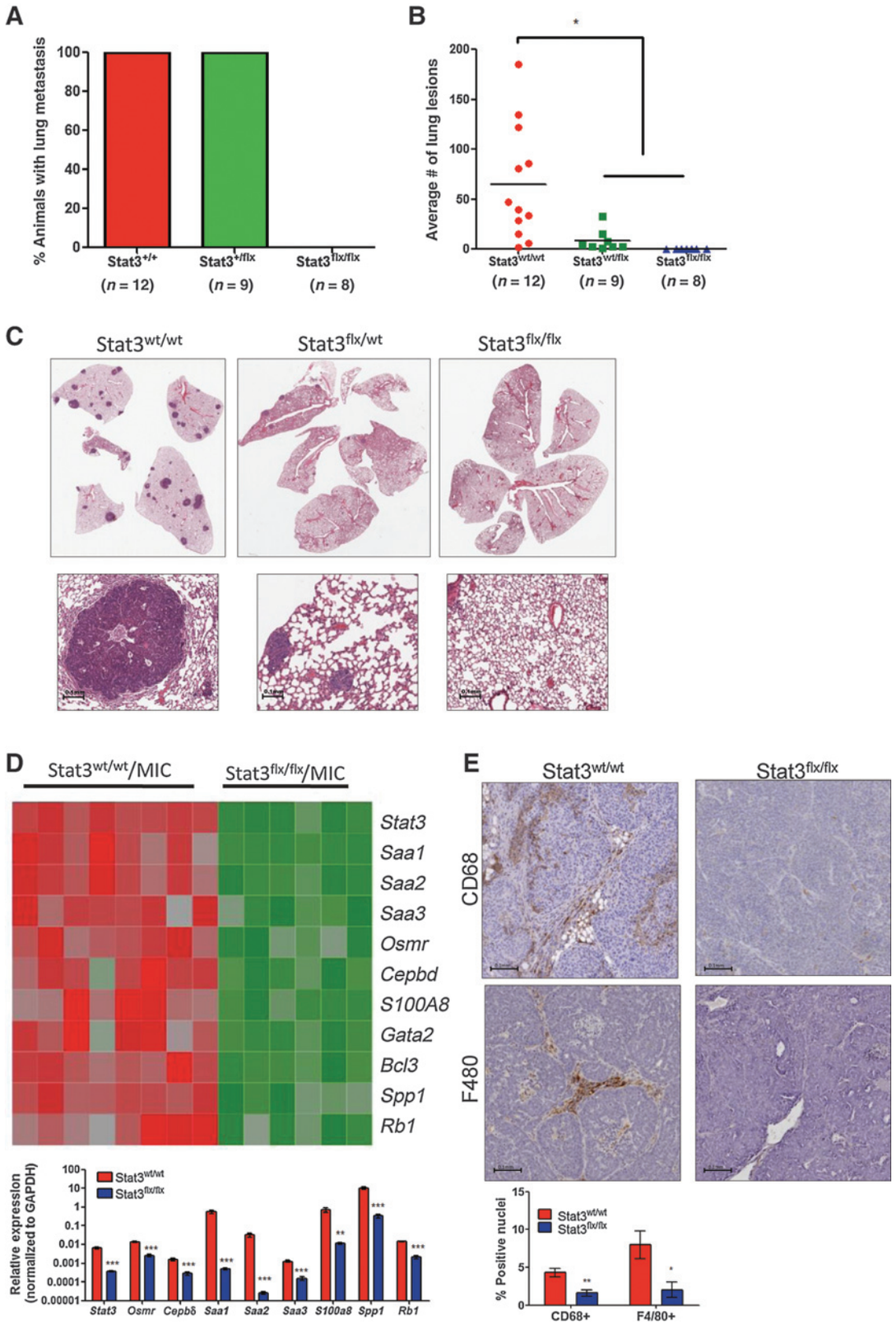

Published OnlineFirst December 30, 2015; DOI: 10.1158/0008-5472.CAN-15-2770

both wild-type and Stat3-deficient tumors with myeloid cell markers CD68 and F4/80. In contrast to the robust immune recruitment, we saw in early Stat3-deficient lesions (Figs. 3 and 4) or end-stage wild-type tumors (Fig. 6E), the Stat3-deficient tumors had a significant reduction in infiltrating $CD68^+$ and $F4/80_+$ populations (Fig. 6E). Furthermore we show that these Stat3-deficient tumors have managed to effectively suppress the immune response as exhibited by low overall leukocyte and T-cell infiltration compared to the wild-type tumors (Supplementary Fig. S3D). Taken together, these results argue that a Stat3-dependent transcription network involved in promoting an inflammatory tumor microenvironment that plays a critical role these tumors' metastatic capacity. Thus, we have demonstrated the importance of tumor epithelial expression of Stat3 in promoting immune suppression during early stages of tumor progression and a prometastatic inflammatory tumor microenvironment in late-stage tumors (Fig. 7). In addition, we propose an interesting model to investigate the mechanisms of immune-mediated tumor elimination.

Discussion

Several studies have highlighted altered tumor immune microenvironments as an important factor in tumor progression and malignancy. Indeed, several studies have shown that an elevated Th1/Th2 ratio is the best predictor of good outcome in patients with invasive breast cancer (6), while others have shown that increased presence of intratumoral macrophages are associated with metastasis and poor outcome (3–5). However, most of these studies have focused on invasive metastatic disease leaving the molecular mechanisms that promote antitumor immunity to prevent the DCIS to invasive ductal carcinoma (IDC) transition poorly defined.

Stat3 has been well characterized as an important player in inflammation and its activation is often dysregulated in human breast cancers (8, 9, 11). Several *in vitro* and a few *in vivo* models have highlighted the importance of Stat3 in tumor growth, invasiveness, and metastasis (11, 12). The recent development of a PyVmT-IRES-Cre mouse model of breast cancer that can be induced in temporal fashion has enabled us to investigate the role of Stat3 throughout all stages of mammary tumor progression. As mammary epithelial–specific expression of PyVmT is dependent on doxycycline, unlike the conventional germline MMTV/PyVmT model, the PyVmT oncogene product is not immunologically tolerized and behaves as a tumor antigen. This unique model has also allowed us to evaluate how tumor epithelial ablation of Stat3 can impact on the tumor immune microenvironment at tumor initiation and progression in a transgenic, immunocompetent context. Furthermore, our model, in the absence of Stat3, nicely recapitulate the 3 phases of immunoediting; elimination, equilibrium, and escape. As we have shown, early Stat3-deficient lesions form to a comparable level to the parental MIC line. However, in the absence of Stat3 these lesions are eliminated by the immune system (Figs. 2–4) followed by a long period of latency, which may be indicative of the equilibrium phase, wherein dormant PyVmT cells continue to reside within these Stat3-deficient mammary glands and are kept in check by the adaptive immune system. Eventually a proportion of these latent PyVmT tumor cells are able to circumvent this equilibrium phase and escape to form detectable tumors (Fig. 1), though they are unable to metastasize to the lung, an observation that correlated with the loss of a proinflammatory tumor microenvironment (Fig. 6).

While Stat3 deletion had little impact on the initial development of mammary epithelial hyperplasias, which retained comparable proliferative and apoptotic potential (Fig. 2A–C), these Stat3-deficient lesions demonstrated a dramatic infiltration of myeloid populations and T-cell infiltrates compared with the parental Stat3-proficient lesions, which eventually led to clearance of these lesions (Fig. 2). Furthermore, we demonstrated that this tumor immune clearance is mediated through a shift away from $CD206^+$ M2-polarized macrophages and an increase in $CD103^+$ DCs and activated CTLs in the absence of epithelial Stat3 (Figs. 3 and 4).

M2-polarized macrophages are thought to play critical role in facilitating breast cancer progression (24, 25). Consistent with these results, epithelial-derived Stat3 has previously been shown to play an important role in the macrophage polarization event, skewing the polarization towards an M2, immunosuppressive state (32). Interesting future directions may include investigating the functional changes in these myeloid cells. By isolating the myeloid cells recruited to these lesions, we could examine differences in their cytokine production, expression of costimulatory molecules and T-cell activation capacity, thus providing additional insight into the mechanism by which they clear the malignant lesions in the absence of Stat3.

Dendritic cells have also come to light as important modulators of tumor immune response (24, 25). The ratio of CD103:CD11b expressing DCs plays a key role in the antitumor activation of $CD8^+$ CTLs and further correlates with better prognosis in human lung and breast cancer (22). Consistent with this, epithelial ablation of Stat3 at early tumor initiation stages results in a higher CD103:CD11b DC ratio (Fig. 3) and an increase in highly activated $CD8^+$ CTLs (Fig. 4). In addition, the Stat3-deficient lesions exhibit a marked increase in their CD8:CD4 ratio, an elevated ratio that correlates with better patient outcome (6).

Further investigation into the molecular mechanism by which Stat3 promotes this immunosuppressive tumor microenvironment is essential. Production of such immunosuppressive factors as IL10, IL23, and TGFβ by Stat3 in a number of hematopoietic lineages has been shown to cause an overall dampening of the immune response (13, 14, 16). Similarly, in the context of the mammary epithelium, Stat3 has been shown to attenuate of the APR, resulting in a decrease in proinflammatory cytokine signalling during mammary gland involution (32) and a Stat3-

Figure 6.

Stat3 modulates expression of inflammatory gene crucial for metastasis to the lungs. A and B, percentage of $Stat3^{wt/wt}$/MTB/MIC, $Stat3^{wt/flx}$/MTB/MIC, and $Stat3^{flx/flx}$/MTB/MIC animals with metastatic lung lesions (A) and quantification of the average number of lesions (B). C, representative H&E images of lung metastases. D, heatmap of selected differentially expressed inflammatory genes between the $Stat3^{wt/wt}$ and $Stat3^{flx/flx}$ end stage tumors by microarray analysis. Differentially expressed genes represent a minimum 2-fold difference and an FDR value of 0.02. Validation of these targets was performed using qRT-PCR and their relative expression displayed. E, staining of paraffin-embedded sections of mammary tumors using antibodies against CD68 (monocyte marker) and F4/80 (macrophage marker) and quantification (*, $P < 0.05$; **, $P < 0.01$; ***, $P < 0.001$). IHC, $n = 8$ biologic replicates per genotype. Scale bar, 100 μm.

Published OnlineFirst December 30, 2015; DOI: 10.1158/0008-5472.CAN-15-2770

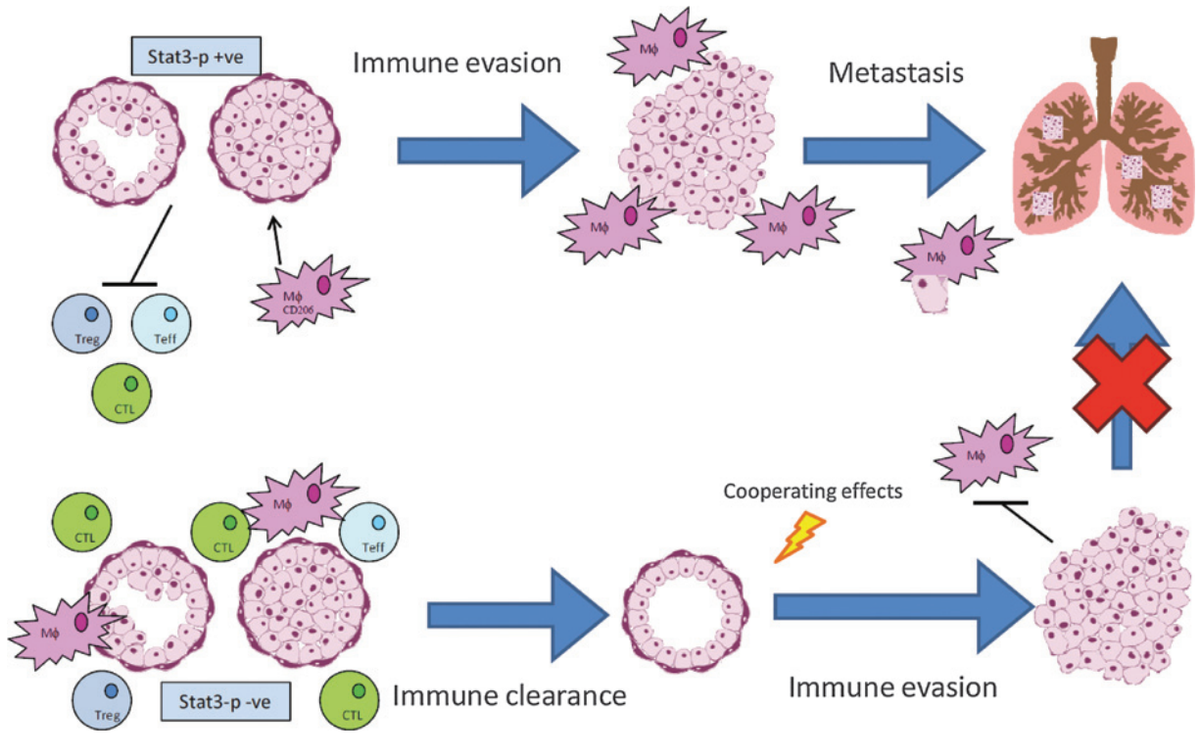

Figure 7.
Stat3 modulates immune response at various stages of tumor progression. Schematic representation of the role of Stat3 in mediating immune evasion and prometastatic inflammation during tumor initiation and progression. During tumor initiation, Stat3 activation results in a suppression of immunosurveillance. As the tumor progresses, it recruits M2 macrophages, which leads to its eventual metastasis. In contrast, in the absence of Stat3, a robust immune response led by activated T cells eliminates early cancerous lesions. This is followed by a long equilibrium period, during which time, cooperating events can occur to result in the escape of a percentage of the tumors. However, Stat3 ablation still results in reduced recruitment of proinflammatory macrophages and an inability to metastasize.

dependent wound healing–like immune program involving IL10 has been identified in the post-partum involuting mammary gland (33). Investigation into a Stat3-dependent cytokine network responsible for establishing this immunosuppressive tumor microenvironment during DCIS to invasive disease transition may have important therapeutic implications.

The importance of T cells in establishing immune surveillance is further supported by the observation that Stat3-deficient hyperplasias and adenomas can be partially rescued by introducing Stat3-deficient PyVmT lesions into a SCID genetic background (Fig. 5). However, even on this SCID genetic background, these hyperplastic lesions were not able to progress to fully invasive adenocarcinomas, indicating that while the T cells play an important role in the immune clearance of these nascent lesions, other components of the innate immune system are involved in suppressing later stages of tumor progression. Natural killer (NK) cells, which remain intact in the SCID mouse, may play an important role in this. A role for NK cells in antitumor immunity has been well documented in various mouse models and their presence has been correlated with better prognosis in some cancers (34). In fact, the presence of molecular signatures of NK cells were shown to be positive predictors of relapse-free survival in a retrospective study of breast cancer patients (35). Therefore, while we have shown that T cells are major effectors of the immune surveillance observed in our model, the roles of the remaining innate immune cells in suppressing tumor growth remain to be elucidated.

Although these studies provide compelling evidence that tumor epithelial expression of Stat3 is involved in suppressing tumor immune surveillance, 30% of the Stat3-deficient MIC animals develop focal mammary tumors that evaded immune surveillance as evidence by the profound loss of immune infiltrate (Fig. 6) and reached the escape phase of the immunoediting program. The precise molecular mechanism by which this occurs remains to be elucidated. Possible mechanisms involved in this escape from immune surveillance involve major changes at either the tumor cell level or that of the tumor microenvironment, although, in general, these mechanisms are not fully understood (2). On the basis of the long latency of these Stat3-deficient tumors, there is opportunity for stochastic genetic or epigenetic alterations to occur, leading to the eventual outgrowth of the mammary tumors. This may result in reduced immunogenicity of the tumors due to downregulation of immunogenic molecules such as the MHC class I and II molecules or resistance to the cytotoxic functions of the immune cells (2). Indeed other genetic alterations could result in the activation of several other transcription factors have been implicated in supporting an immunosuppressive environment including NF-κB, AP-1, and SMAD (36). Alternatively, this tumor escape could be the result of peripheral tolerance against the PyVmT antigen from $CD8^+$ T-cell anergy or deletion as shown by Willimsky and colleagues using a sporadically expressed dormant viral Tag oncogene (37). Thus, while there is evidence of possible mechanisms to explain

this escape, the precise mechanisms in play in our model have yet to be determined.

Despite the capacity to eventually escape immune surveillance, the Stat3-deficient tumors were incapable of metastasizing to the lungs. Consistent with the importance of Stat3 in the metastatic phase of tumor progression, we have previously demonstrated that Stat3 ablation in an ErbB2 model of breast cancer resulted in a similar metastatic blockade (12). Interestingly, in both models, gene expression analyses revealed the downregulation of a Stat3-dependent inflammatory transcriptional network involving *Saa1*, *Saa2*, *Saa3*, *S100a8*, *Cepbδ*, and *Osmr* and implicates it in the metastatic program (12). Indeed, elevated expression of OSMR has been correlated with poor prognosis in several cancers (38). In addition, SAA3 and S100A8 expression at both the primary tumor site and premetastatic niche facilitates myeloid cell recruitment and metastasis (39–41). Consistent with this concept, the Stat3-deficient PyVmT tumors exhibit a marked deficit in TAMs (Fig. 6). Given the importance of macrophage recruitment to primary tumor site in metastasis (7, 42) these data indicate that Stat3 plays a critical role in promoting a metastatic tumor microenvironment.

These observations have several important implications in the therapeutic management of metastatic breast cancers. The observation that Stat3 plays a critical role in suppressing immune surveillance raises the intriguing possibility that small-molecule inhibitors targeting Stat3 may be effective agents to reactivate the immune surveillance program. Interesting combinatory studies looking at Stat3 inhibition along with new immunostimulatory treatments such as anti-PDL1 and anti-CTL4 antibody therapies may also prove efficacious in mobilizing antitumor immune response. Further studies into the mechanism of this Stat3-mediated immune evasion may greatly benefit the current research into various immunotherapies or support the role for direct Stat3 inhibitors in both early and metastatic breast cancers.

Disclosure of Potential Conflicts of Interest

No potential conflicts of interest were disclosed.

Authors' Contributions

Conception and design: L.M. Jones, J.J. Ranger, W.J. Muller
Development of methodology: L.M. Jones, J.J. Ranger, J. Ursini-Siegel, M. Krummel
Acquisition of data (provided animals, acquired and managed patients, provided facilities, etc.): L.M. Jones, M.L. Broz, J.J. Ranger, R. Ahn
Analysis and interpretation of data (e.g., statistical analysis, biostatistics, computational analysis): L.M. Jones, M.L. Broz, J.J. Ranger, J. Ozcelik, J. Ursini-Siegel, M.T. Hallett, M. Krummel, W.J. Muller
Writing, review, and/or revision of the manuscript: L.M. Jones, M.L. Broz, J.J. Ranger, M. Krummel, W.J. Muller
Administrative, technical, or material support (i.e., reporting or organizing data, constructing databases): L.M. Jones, R. Ahn, D. Zuo
Study supervision: J.J. Ranger, W.J. Muller

Acknowledgments

The authors thank Vasilios Papavasiliou and Cynthia Lavoie for technical support and Dr. Connie Krawczyk for helpful discussion.

Grant Support

This work was supported by the Terry Fox Frontier Program Project Team Grant (020002), McGill Integrated Cancer Research Training Program Fellowship and McGill University Health Center Studentship (L.M. Jones), McGill University Canadian Research Chair in Molecular Oncology (W.J. Muller), Genentech Predoctoral Research Fellowship, the Margaret A. Cunningham Immune Mechanisms in Cancer Research Fellowship Award, and the Achievement Reward for College Scientists Scholarship (M. Broz), NIH grants U54 CA163123 and R21CA191428 (M. Krummel), and Canadian Cancer Society (grant 702060; J. Ursini-Siegel).

The costs of publication of this article were defrayed in part by the payment of page charges. This article must therefore be hereby marked *advertisement* in accordance with 18 U.S.C. Section 1734 solely to indicate this fact.

Received October 13, 2015; revised December 8, 2015; accepted December 21, 2015; published OnlineFirst December 30, 2015.

References

1. Dunn GP, Bruce AT, Ikeda H, Old LJ, Schreiber RD. Cancer immunoediting: from immunosurveillance to tumor escape. Nat Immunol 2002;3:991–8.
2. Smyth MJ, Dunn GP, Schreiber RD. Cancer immunosurveillance and immunoediting: the roles of immunity in suppressing tumor development and shaping tumor immunogenicity. Adv Immunol 2006;90:1–50.
3. DeNardo DG, Andreu P, Coussens LM. Interactions between lymphocytes and myeloid cells regulate pro- versus anti-tumor immunity. Cancer Metastasis Rev 2010;29:309–16.
4. Leek RD, Hunt NC, Landers RJ, Lewis CE, Royds JA, Harris AL. Macrophage infiltration is associated with VEGF and EGFR expression in breast cancer. J Pathol 2000;190:430–6.
5. Tsutsui S, Yasuda K, Suzuki K, Tahara K, Higashi H, Era S. Macrophage infiltration and its prognostic implications in breast cancer: the relationship with VEGF expression and microvessel density. Oncol Rep 2005;14:425–31.
6. Kristensen VN, Vaske CJ, Ursini-Siegel J, Van Loo P, Nordgard SH, Sachidanandam R, et al. Integrated molecular profiles of invasive breast tumors and ductal carcinoma in situ (DCIS) reveal differential vascular and interleukin signaling. Proc Natl Acad Sci U S A 2012;109:2802–7.
7. DeNardo DG, Barreto JB, Andreu P, Vasquez L, Tawfik D, Kolhatkar N, et al. CD4(+) T cells regulate pulmonary metastasis of mammary carcinomas by enhancing protumor properties of macrophages. Cancer Cell 2009;16:91–102.
8. Hsieh FC, Cheng G, Lin J. Evaluation of potential Stat3-regulated genes in human breast cancer. Biochem Biophys Res Commun 2005;335:292–9.
9. Diaz N, Minton S, Cox C, Bowman T, Gritsko T, Garcia R, et al. Activation of stat3 in primary tumors from high-risk breast cancer patients is associated with elevated levels of activated SRC and survivin expression. Clin Cancer Res 2006;12:20–8.
10. Yu H, Lee H, Herrmann A, Buettner R, Jove R. Revisiting STAT3 signalling in cancer: new and unexpected biological functions. Nat Rev Cancer 2014;14:736–46.
11. Sansone P, Bromberg J. Targeting the interleukin-6/Jak/stat pathway in human malignancies. J Clin Oncol 2012;30:1005–14.
12. Ranger JJ, Levy DE, Shahalizadeh S, Hallett M, Muller WJ. Identification of a Stat3-dependent transcription regulatory network involved in metastatic progression. Cancer Res 2009;69:6823–30.
13. Yu H, Kortylewski M, Pardoll D. Crosstalk between cancer and immune cells: role of STAT3 in the tumour microenvironment. Nat Rev Immunol 2007;7:41–51.
14. Kortylewski M, Kujawski M, Wang T, Wei S, Zhang S, Pilon-Thomas S, et al. Inhibiting Stat3 signaling in the hematopoietic system elicits multicomponent antitumor immunity. Nat Med 2005;11:1314–21.
15. Wu L, Du H, Li Y, Qu P, Yan C. Signal transducer and activator of transcription 3 (Stat3C) promotes myeloid-derived suppressor cell expansion and immune suppression during lung tumorigenesis. Am J Pathol 2011;179:2131–41.
16. Ferguson SD, Srinivasan VM, Heimberger AB. The role of STAT3 in tumor-mediated immune suppression. J Neurooncol 2015;123:385–94.
17. Kortylewski M, Yu H. Role of Stat3 in suppressing anti-tumor immunity. Curr Opin Immunol 2008;20:228–33.
18. Raz R, Lee CK, Cannizzaro LA, d'Eustachio P, Levy DE. Essential role of STAT3 for embryonic stem cell pluripotency. Proc Natl Acad Sci U S A 1999;96:2846–51.

Published OnlineFirst December 30, 2015; DOI: 10.1158/0008-5472.CAN-15-2770

19. Rao T, Ranger JJ, Smith HW, Lam SH, Chodosh L, Muller WJ. Inducible and coupled expression of the polyomavirus middle T antigen and Cre recombinase in transgenic mice: an in vivo model for synthetic viability in mammary tumour progression. Breast Cancer Res 2014;16:R11.
20. Gunther EJ, Belka GK, Wertheim GB, Wang J, Hartman JL, Boxer RB, et al. A novel doxycycline-inducible system for the transgenic analysis of mammary gland biology. FASEB J 2002;16:283–92.
21. Movahedi K, Laoui D, Gysemans C, Baeten M, Stange G, Van den Bossche J, et al. Different tumor microenvironments contain functionally distinct subsets of macrophages derived from Ly6C(high) monocytes. Cancer Res 2010;70:5728–39.
22. Broz ML, Binnewies M, Boldajipour B, Nelson AE, Pollack JL, Erle DJ, et al. Dissecting the tumor myeloid compartment reveals rare activating antigen-presenting cells critical for T cell immunity. Cancer Cell 2014;26:638–52.
23. Mantovani A, Sica A, Sozzani S, Allavena P, Vecchi A, Locati M. The chemokine system in diverse forms of macrophage activation and polarization. Trends Immunol 2004;25:677–86.
24. Woo SR, Corrales L, Gajewski TF. Innate immune recognition of cancer. Annu Rev Immunol 2015;33:445–74.
25. Hagerling C, Casbon AJ, Werb Z. Balancing the innate immune system in tumor development. Trends Cell Biol 2015;25:214–20.
26. Bosma MJ, Carroll AM. The SCID mouse mutant: definition, characterization, and potential uses. Annu Rev Immunol 1991;9:323–50.
27. Grimm SL, Rosen JM. The role of C/EBPbeta in mammary gland development and breast cancer. J Mammary Gland Biol Neoplasia 2003;8:191–204.
28. Cantwell CA, Sterneck E, Johnson PF. Interleukin-6-specific activation of the C/EBPdelta gene in hepatocytes is mediated by Stat3 and Sp1. Mol Cell Biol 1998;18:2108–17.
29. Ray A, Ray BK. Serum amyloid A gene expression under acute-phase conditions involves participation of inducible C/EBP-beta and C/EBP-delta and their activation by phosphorylation. Mol Cell Biol 1994;14:4324–32.
30. Hagihara K, Nishikawa T, Sugamata Y, Song J, Isobe T, Taga T, et al. Essential role of STAT3 in cytokine-driven NF-kappaB-mediated serum amyloid A gene expression. Genes Cells 2005, 10:1051–63.
31. Liu MJ, Bao S, Napolitano JR, Burris DL, Yu L, Tridandapani S, et al. Zinc regulates the acute phase response and serum amyloid A production in response to sepsis through JAK-STAT3 signaling. PLoS One 2014;9:e94934.
32. Hughes K, Wickenden JA, Allen JE, Watson CJ. Conditional deletion of Stat3 in mammary epithelium impairs the acute phase response and modulates immune cell numbers during post-lactational regression. J Pathol 2012;227:106–17.
33. Martinson HA, Jindal S, Durand-Rougely C, Borges VF, Schedin P. Wound healing-like immune program facilitates postpartum mammary gland involution and tumor progression. Int J Cancer 2015;136:1803–13.
34. Waldhauer I, Steinle A. NK cells and cancer immunosurveillance. Oncogene 2008;27:5932–43.
35. Ascierto ML, Idowu MO, Zhao Y, Khalak H, Payne KK, Wang XY, et al. Molecular signatures mostly associated with NK cells are predictive of relapse free survival in breast cancer patients. J Transl Med 2013;11:145.
36. Grivennikov SI, Greten FR, Karin M. Immunity, inflammation, and cancer. Cell 2010;140:883–99.
37. Willimsky G, Blankenstein T. Sporadic immunogenic tumours avoid destruction by inducing T-cell tolerance. Nature 2005;437:141–6.
38. Savarese TM, Campbell CL, McQuain C, Mitchell K, Guardiani R, Quesenberry PJ, et al. Coexpression of oncostatin M and its receptors and evidence for STAT3 activation in human ovarian carcinomas. Cytokine 2002;17:324–34.
39. Gebhardt C, Nemeth J, Angel P, Hess J. S100A8 and S100A9 in inflammation and cancer. Biochem Pharmacol 2006;72:1622–31.
40. Hsu K, Chung YM, Endoh Y, Geczy CL. TLR9 ligands induce S100A8 in macrophages via a STAT3-dependent pathway which requires IL-10 and PGE2. PLoS One 2014;9:e103629.
41. Hiratsuka S, Watanabe A, Sakurai Y, Akashi-Takamura S, Ishibashi S, Miyake K, et al. The S100A8-serum amyloid A3-TLR4 paracrine cascade establishes a pre-metastatic phase. Nat Cell Biol 2008;10:1349–55.
42. Lin EY, Jones JG, Li P, Zhu L, Whitney KD, Muller WJ, et al. Progression to malignancy in the polyoma middle T oncoprotein mouse breast cancer model provides a reliable model for human diseases. Am J Pathol 2003;163:2113–26.

Published OnlineFirst December 30, 2015; DOI: 10.1158/0008-5472.CAN-15-2770

Cancer Research
The Journal of Cancer Research (1916–1930) | The American Journal of Cancer (1931–1940)

AACR American Association for Cancer Research

STAT3 Establishes an Immunosuppressive Microenvironment during the Early Stages of Breast Carcinogenesis to Promote Tumor Growth and Metastasis

Laura M. Jones, Miranda L. Broz, Jill J. Ranger, et al.

Cancer Res 2016;76:1416-1428. Published OnlineFirst December 30, 2015.